Published by IOP Publishing for Sissa Medialab

Received: *January 14, 2020*
Accepted: *March 2, 2020*
Published: *April 8, 2020*

XII International Symposium on Radiation from Relativistic Electrons in Periodic Structures — RREPS-19
September 16–20, 2019
Belgorod, Russian Federation

2020 JINST 15 C04023

Influence of 3D-printed collimator thickness on near-the-edge scattering of high-energy electrons

S.G. Stuchebrov,[a] A.A. Bulavskaya,[a] Yu.M. Cherepennikov,[a] E. Gargioni,[b] A.A. Grigorieva[a,1] and I.A. Miloichikova[a,c]

[a] *National Research Tomsk Polytechnic University, Lenin Avenue 30, Tomsk, 634050, Russian Federation*
[b] *University Medical Center Hamburg-Eppendorf, Martinistrasse 52, Hamburg, 20246, Germany*
[c] *Cancer Research Institute of Tomsk NRMC RAS, Kooperativny Street 5, Tomsk, 634050, Russian Federation*

E-mail: anngrigorievabr@gmail.com

Abstract: In this research, we study how the thickness of a 3D-printed collimator affects high-energy electron scattering. As part of this work, an ABS plastic absorber was produced by fused deposition modeling. Dose distributions at the boundary of the plastic absorber were experimentally observed for 6, 12, and 20 MeV electron beams. For plastic absorber thicknesses of up to 3 cm, dose "hot spots" are observed at the boundary between the primary beam and the beam that has passed through the absorber for 12 and 20 MeV electrons. However, no additional scattering is observed at the absorber edges for the thicknesses of plastic collimators above the minimum thickness providing the total absorption of electron beams ($\geq$ 4 cm for 6 MeV electrons, $\geq$ 8 cm for 12 MeV electrons, and $\geq$ 10 cm for 20 MeV electrons). The experiments show that 3D printing is a useful tool for modulating high energy electron beams, for example, in the field of medical physics.

Keywords: Accelerator Applications; Beam dynamics

[1]Corresponding author.

https://doi.org/10.1088/1748-0221/15/04/C04023

Contents

2020 JINST 15 C04023

1 Introduction

Radiation therapy with electron beams is an effective treatment of malignant tumors located on the skin or in the underlying tissues [1]. The main advantage of electron beam therapy is the opportunity to regulate the depth of beam penetration by varying the beam energy. This provides more homogenous dose distributions in the target volume and a significant reduction in healthy organs and tissues exposure to radiation [2].

Higher requirements for the accuracy of dose delivery in radiation therapy makes it relevant to create patient-specific beam shaping elements, such as collimators. Patient-specific collimators can shape dose fields of complex geometry corresponding to the tumor contour obtained from the patients' tomography data [3]. The advancement of this approach in clinical practice is stifled by high requirements to the working premises, operating conditions, and qualification of the staff, when it comes to metal casting for medical collimators [4], which are, moreover, toxic and cost inefficient.

Research into the 3D printing technology to produce patient-specific samples for medical purposes has become increasingly topical over the last decade [5, 6]. Particularly, this approach is used to produce boluses for radiation therapy with electron [7, 8] and photon beams [9], as well as applicators for brachytherapy [10] and immobilization devices [11].

In our previous research [12], we proposed 3D-printing patient-specific collimators and showed that this solution does not have the limitations typical of the approaches based on metal melting and casting and, at the same time, allows for efficient absorption of high-energy electrons.

The next step to determine the applicability of this solution in radiation therapy, is to investigate how the thickness of the 3D-printed collimator affects the high-energy electron scattering.

2 Methods and materials

2.1 Test samples

In this research, we study how the thickness of plastic absorbers affects the electron scattering at the edge of the sample. The 3D models of test samples were designed so that the absorber thickness

ranged from 1 to 15 cm with a step of 1 cm. Figure 1 shows 3D models of the test objects. The transverse size of both samples is $2 \times 3\,\mathrm{cm}^2$.

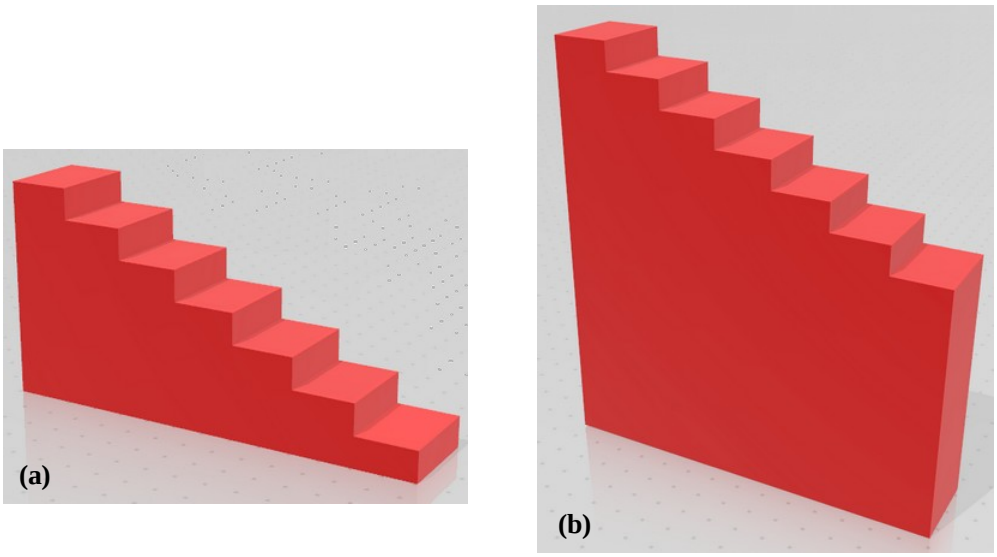

Figure 1. 3D models of plastic absorbers: (a) 1 to 7 cm thick, (b) 8 to 15 cm thick.

The absorbers were produced by fused deposition modeling, which is the most popular and affordable choice [13]. It involves heating thermoplastics to their melting point, and extruding them through a nozzle on the substrate layer by layer. The layers stick together while cooling. This technology can print samples with a complex geometry from harmless thermoplastics [14].

A wide variety of polymers can be used for 3D printing. However, the most widespread ones are acrylonitrile butadiene styrene (ABS), polylactide (PLA), high impact polystyrene (HIPS), and polyamide (PA), also known as nylon [13]. In this research, we investigated the readily available ABS plastic, which can be used to 3D-print of large-sized samples without mechanical defects [13].

Test samples were made of ABS plastic filament produced by Bestfilament [15] using a Prism Pro 3D printer [16]. The following printing parameters were used for this work: 1.75 mm filament diameter, 0.3 mm layer thickness, 0.4 mm nozzle diameter, 40 mm per minute printing speed, 235°C nozzle temperature, 90°C desk temperature, and 100% filling coefficient.

2.2 Experimental setup

A TrueBeam 2.0 clinical linear accelerator (Varian Medical Systems Inc., Palo Alto, California, United States) [17] mounted at the University Medical Center Hamburg-Eppendorf (UKE, Hamburg, Germany) was used as an electron source. The electron energies in the experiments were set at 6, 12, and 20 MeV. Figure 2 shows experimental scheme.

A printed plastic sample was installed in the center of a standard $15 \times 15\,\mathrm{cm}^2$ square applicator. GAFCHROMIC EBT 3 dosimetry films were used to measure the dose field distribution [18]. Dosimetry films were located on the surface of an I'mRT Phantom, which is composed of RW3 material [19]. The source to phantom surface distance was kept at 100 cm, and the sample front edge to surface distance was 6.3 cm. During the experiment, a 2 Gy dose was delivered to the dose-maximum depth for each electron beam energy. Dosimetry films were positioned so that the

2020 JINST 15 C04023

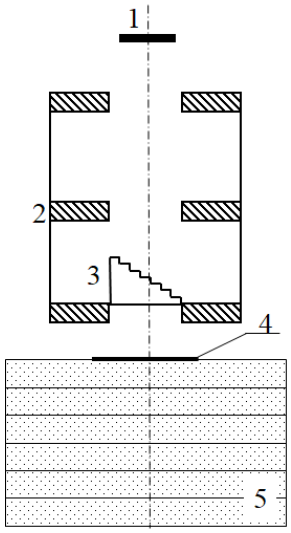

Figure 2. Experimental scheme: 1 — electron source, 2 — standard metal applicator, 3 — 3D printed plastic sample, 4 — dosimetry film, 5 — tissue-equivalent solid phantom.

stair-shaped element of the plastic absorber with chosen thicknesses fully covered one part of the film, while the other part was exposed to the primary beam.

The dose distributions registered by dosimetry films were digitalized using an Epson Perfection V 750 PRO scanner, recommended by the film manufacturer [20], and mathematically processed using MatLab [21]. Some articles [18, 22] show that the maximum optical density measurement error, caused by film inhomogeneity, is about 5%. Therefore, this value is assumed as the maximum measurement error of the electron dose in our experiments.

3 Results and discussions

In order to study the electron scattering effect at the edge of the ABS absorber, we analyzed the dose profile at the boundary between the primary beam and the one passing through the absorber. Our previous research [12] has shown the electron beams of 6, 12, and 20 MeV are completely absorbed when the ABS plastic absorber is at least 4.0 cm, 7.5 cm, and 10.5 cm thick, respectively. The electron beam is considered completely absorbed when the dose level does not exceed the background value.

Figure 3 shows the dose profiles for a 6 MeV electron beam with the plastic absorber thickness ranging from 1 to 5 cm, respectively, with a step of 1 cm. The zero point on the x-axis corresponds to the location of the absorber edge. The dose value is normalized to the primary beam dose.

It can be observed (figure 3) that the curve on the left, which corresponds to film locations below the absorber, does not fall to zero for low thickness (1, 2 cm), because the beam is not completely absorbed by the sample and, therefore, the electrons that have passed through it contribute to the dose. That is why the dose value for a 1 cm absorber is higher than for a 2 cm one. However, when the thickness of the absorber approaches 4 cm, which allows for the total absorption of 6 MeV electron beam, the dose gradient becomes higher. Moreover, for thicknesses exceeding 4 cm, the curves coincide. This means that exceeding the total absorption thickness has no additional contribution

2020 JINST 15 C04023

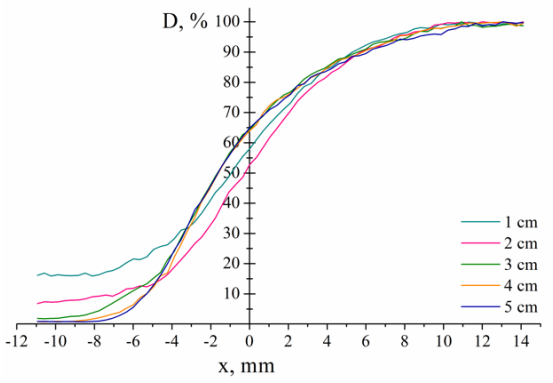

Figure 3. Dose distribution at the absorber edge under 6 MeV electron beam irradiation for different absorber thicknesses. The zero point on the x-axis corresponds to the location of the absorber edge, negative coordinates corresponds to points below the absorber.

to the electron scattering at the edge of the sample. The distance between 80% and 20% isodose curves is 6.7 mm for both 4 and 5 cm absorbers.

Figure 4 shows similar curves for 12 and 20 MeV electron beams. In this case, the thicknesses of the plastic absorbers were varied from 2 to 10 cm with a step of 2 cm for a 12 MeV beam, and from 2 to 15 cm with a step of 3 cm for a 20 MeV beam, respectively. The zero point on the x-axis corresponds to the location of the absorber edge. The dose value is normalized to the primary beam dose.

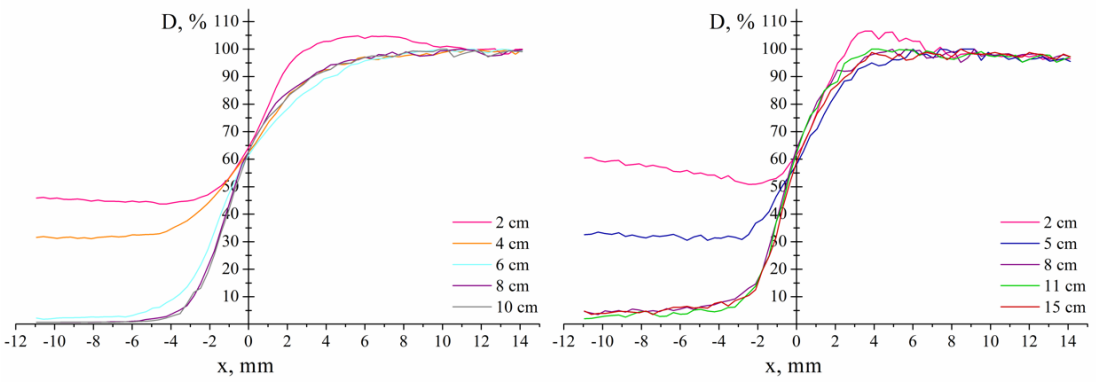

(a) **(b)**

Figure 4. Dose profile at the absorber edge under 12 MeV (a) and 20 MeV (b) electron beam irradiation for different absorber thicknesses. The zero point on the x-axis corresponds to the location of the absorber edge, negative co-ordinates corresponds to points below the absorber.

Curves in figure 4 demonstrate a similar behavior to that of the curves for a 6 MeV beam (figure 3), when the thickness of the absorber approaches the total absorption value (namely, 7.5 cm for 12 MeV, and 10.5 cm for 20 MeV). A few studies proved high sensitivity of GAFCHROMIC EBT 3 dosimetry films to different kind of radiation [23, 18]. It was demonstrated that these dosimetry films can be used to measure electron or mixed photon/electron dose distributions [18]. Low background measured by GAFCHROMIC EBT 3 dosimetry film for 8, 11, and 15 cm sample thick-

2020 JINST 15 C04023

nesses (figure 4b, purple, green, and red lines) for a 20 MeV beam is caused by high-energy gamma radiation generated when high-energy electrons interact with the sample and not absorbed by the plastic. It should be noted that background bremsstrahlung is generated by electron interaction with both collimation system and irradiated object (patient, phantom etc.). Currently, bremsstrahlung contribution to the dose for modern accelerators is estimated as 0.5–5.0% for electron beams with energies of 6–20 MeV [4].

The distance between 80% and 20% isodose curves equals 3.5 mm for a 12 MeV beam and 3 mm for a 20 MeV beam, thus showing a higher dose gradient at the boundary between the primary beam and the one passing through the absorber when the beam energy is higher (figure 4).

For low thicknesses, "hot spots" are observed near the absorber edge under the primary beam and "cold spots" under the absorber (see the 2 cm thickness curve in figure 4), which is not observed for a 6 MeV beam. To investigate this effect in more detail, dose distributions at the absorber edges are studied for 12 and 20 MeV electron beams, where the absorber thicknesses are varied from 1 to 5 cm with a step of 1 cm (figure 5).

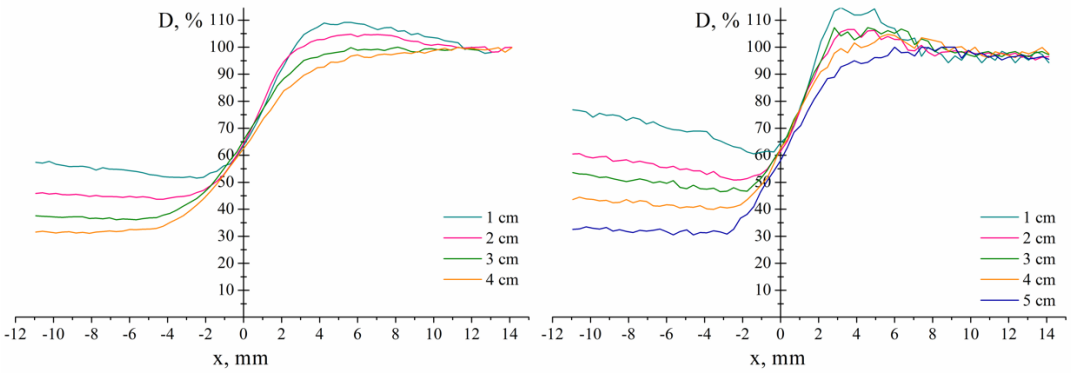

Figure 5. Dose distribution at the absorber edge under 12 MeV (a) and 20 MeV (b) electron beam irradiation for different absorber thicknesses.

Figure 5 shows that hot and cold spots can be observed at the sample edge for the thicknesses of up to 3 cm and the energy of 12 MeV or for the thicknesses of up to 4 cm and the energy of 20 MeV. This "dose transfer" to the primary beam is caused by the high-energy electrons that scatter in the sample near its edge and are capable of escaping and therefore of contributing to the primary beam fluence. This phenomenon can be assessed by observing figure 6, which shows the electron mean free path ($\langle\lambda\rangle$) in air and plastic versus electron energy. These data were calculated based on results of numerical simulation of electron beam propagation in media with macroscopic parameters maximally close to ones of experimentally investigated materials.

Figure 6 demonstrates a sharp decrease in the distance between particle collisions when the electron energy goes below 5 MeV. Although electrons lose energy in small portions in the interactions, just a few collisions are enough for 6 MeV electrons to reach the energy when scattering increases sharply, while 12 and 20 MeV electrons need multiple collisions for that.

When the electron energy is high and the sample is thin, the particle path in the air is not long enough to provide significant scattering: it is only about a few dozens of mean free paths.

2020 JINST 15 C04023

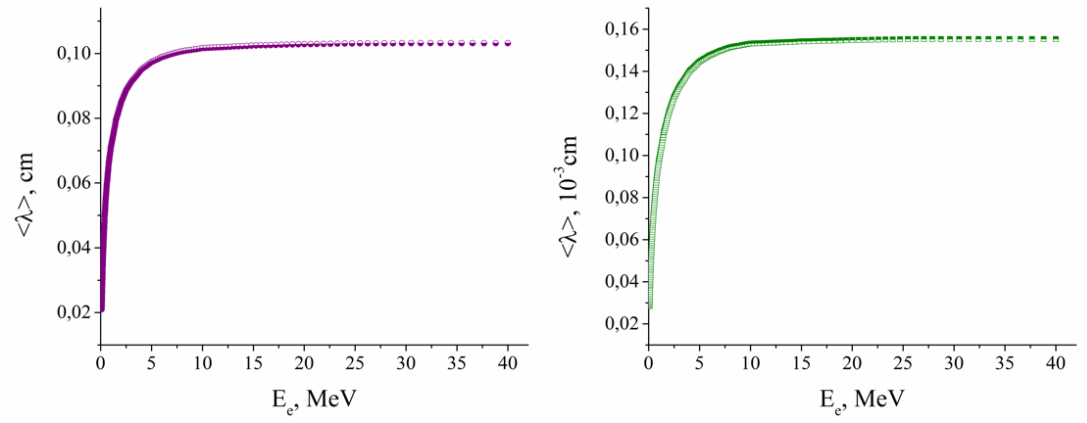

Figure 6. Electron mean free path ($\langle\lambda\rangle$) in air (a) and ABS plastic (b) versus electron energy.

In this case, the electrons are highly unlikely to escape from the air to the plastic sample, while the reverse process (electrons escaping from the collimator to the air) is quite possible. This effect disappears with a decrease in the electron energy (see figure 6), an increase in the sample thickness, and, consequently, a longer path in the air, in which electrons are scattered. This dose-transfer effect should be accounted for in the development of forming samples of low thicknesses, such as compensators. Bagne et al. [24] investigated the heterogeneous electron beam profile at the edges of an applicator. They demonstrated that the percent horn relative to the central axis decreases when size of the field entering the applicator approaches the collimation hole size and increases with growing beam energy [24]. Park et al. [25] and Northey et al. [26], moreover, performed numerical simulations modeling the parameters of energy degraders [25] and plastic inserts [26] that are necessary to lower the dose profile horns and reach the predetermined field homogeneity level. They found that optimally shaped additional forming samples provide control of radiation field parameters such as penetration and flatness.

4 Summary

In this research, we investigated how the thickness of a plastic sample affects electron beam scattering. We considered therapeutic electron beams with energies of 6, 12, and 20 MeV, respectively. The research findings indicate that the dose gradient increases at the sample edge with an increase in its thickness. This remains true until the total absorption thickness is reached (4 cm for 6 MeV, 7.5 cm for 12 MeV, and 10.5 cm for 20 MeV). With a further increase in the absorber thickness, the dose distribution curve does not change its shape. Results of this work shows possibility of 3D printed plastic samples application for electron beams collimation.

As part of this research, we also investigated the dose transfer of scattered electrons at the edge of a plastic sample. This effect can be observed for thicknesses of up to 3 cm when the electron energy is 12 MeV and up to 4 cm for 20 MeV electrons. This effect should be accounted for when plastic samples are used, for instance, as compensators.

2020 JINST 15 C04023

Acknowledgments

This work is financially supported by the Russian Science Foundation, project No. 18-79-10052.

References

[1] D.E. Gerber and T.A. Chan, *Recent advances in radiation therapy*, *Am. Fam. Physician* **78** (2008) 1254.

[2] C. Garibaldi, B.A. Jereczek-Fossa, G. Marvaso, S. Dicuonzo, D.P. Rojas, F. Cattani et al., *Recent advances in radiation oncology*, *ecancermedicalscience* **11** (2017) 785.

[3] K.R. Hogstrom and P.R. Almond, *Review of electron beam therapy physics*, *Phys. Med. Biol.* **51** (2006) R455.

[4] F.M. Khan and J.P. Gibbons, *The physics of radiation therapy*, Lippincott Williams & Wilkins (2014).

[5] Q. Yan, H. Dong, J. Su, J. Han, B. Song, Q. Wei et al., *A review of 3d printing technology for medical applications*, *Engineering* **4** (2018) 729.

[6] Y. Zhao, K. Moran, M. Yewondwossen, J. Allan, S. Clarke, M. Rajaraman et al., *Clinical applications of 3-dimensional printing in radiation therapy*, *Med. Dosim.* **42** (2017) 150.

[7] S. Su, K. Moran and J.L. Robar, *Design and production of 3d printed bolus for electron radiation therapy*, *J. Appl. Clin. Med. Phys.* **15** (2014) 194.

[8] M. Łukowiak et al. *Utilization of a 3D printer to fabricate boluses used for electron therapy of skin lesions of the eye canthi*, *J. Appl. Clin. Med. Phys.* **18** (2017) 76.

[9] W. Zou, T. Fisher, M. Zhang, L. Kim, T. Chen, V. Narra et al., *Potential of 3d printing technologies for fabrication of electron bolus and proton compensators*, *J. Appl. Clin. Med. Phys.* **16** (2015) 90.

[10] B.D. Harris, S. Nilsson and C.M. Poole, *A feasibility study for using ABS plastic and a low-cost 3d printer for patient-specific brachytherapy mould design*, *Australas. Phys. Eng. S.* **38** (2015) 399.

[11] M.F. Haefner, F.L. Giesel, M. Mattke, D. Rath, M. Wade, J. Kuypers et al., *3d-printed masks as a new approach for immobilization in radiotherapy — a study of positioning accuracy*, *Oncotarget* **9** (2018) 6490.

[12] I. Miloichikova, A. Bulavskaya, Y. Cherepennikov, B. Gavrikov, E. Gargioni, D. Belousov et al., *Feasibility of clinical electron beam formation using polymer materials produced by fused deposition modeling*, *Phys. Med.* **64** (2019) 188.

[13] A.K. France, *Make: 3D Printing: The Essential Guide to 3D Printers*, Maker Media, Inc. (2013).

[14] A. Boschetto and L. Bottini, *Accuracy prediction in fused deposition modeling*, *Int. J. Adv. Manufact. Technol.* **73** (2014) 913.

[15] https://bestfilament.ru/abs-1-1.75-white/.

[16] https://www.3dquality.ru/catalog/product/3d-printer-prism-pro-v2/.

[17] https://www.varian.com/products/radiotherapy/treatment-delivery/truebeam

[18] P. Sipilä et al., *Gafchromic EBT3 film dosimetry in electron beams — energy dependence and improved film read out*, *J. Appl. Clin. Med. Phys.* **17** (2016) 360.

[19] https://www.iba-dosimetry.com/product/imrt-phantom/.

[20] https://files.support.epson.com/pdf/prv7ph/prv7phug.pdf.

2020 JINST 15 C04023

[21] https://uk.mathworks.com/products/matlab.html.

[22] S. Devic, J. Seuntjens, G. Hegyi, E.B. Podgorsak, C.G. Soares, A.S. Kirov et al., *Dosimetric properties of improved GafChromic films for seven different digitizers*, *Med. Phys.* **31** (2004) 2392.

[23] J. Sorriaux, A. Kacperek, S. Rossomme, J. Lee, D. Bertrand, S. Vynckier et al., *Evaluation of gafchromic® EBT3 films characteristics in therapy photon, electron and proton beams*, *Phys. Med.* **29** (2013) 599.

[24] F.R. Bagne, N. Samsami and R.R. Dobelbower, *Radiation contamination and leakage assessment of intraoperative electron applicators*, *Med. Phys.* **15** (1988) 530.

[25] J.I. Park, S.W. Ha, J. in Kim, H. Lee, J. Lee, I.H. Kim et al., *Design and evaluation of electron beam energy degraders for breast boost irradiation*, *Radiat. Oncol.* **11** (2016) 112.

[26] B.J. Northey and S.F. Zavgorodni, *Optimisation of electron cone design in high energy radiotherapy using the monte carlo method*, *Australas. Phys. Eng. S.* **25** (2002) 7.

2020 JINST 15 C04023